Polímeros
ISSN 1678-5169 (Online)

https://doi.org/10.1590/0104-1428.20240104

ORIGINAL ARTICLES

Synthesis of well-defined polypeptide-based diblock copolymers

Thuy Thu Truong[1,2,3]*, Luan Thanh Nguyen[1,3,4], Tin Chanh Duc Doan[3,4], Le-Thu Thi Nguyen[1,2,3] and Ha Tran Nguyen[1,2,3]*

[1]National Key Laboratory of Polymer and Composite Materials, Ho Chi Minh City, Vietnam
[2]Ho Chi Minh City University of Technology – HCMUT, District 10, Ho Chi Minh City, Vietnam
[3]Vietnam National University, Ho Chi Minh City, Vietnam
[4]Institute for Nanotechnology – INT, Vietnam National University, Thu Duc District, Ho Chi Minh City, Vietnam
**trtthuy@hcmut.edu.vn; nguyentranha@hcmut.edu.vn*

Abstract

We report an efficient protocol to synthesize rod-coil diblock copolymers of an α-helical polypeptide and poly(4-vinyl pyridine) via a combination of "living" ring-opening polymerization of α-amino acid N-carboxyanhydrides at 0 °C, polymer end-group modification and atom transfer radical polymerization (ATRP) of 4-vinyl pyridine (4-VP). Due to the competent effect of the pyridine groups with the ATRP ligand and the low initiation efficacy of the rigid polypeptide macroinitiator at mild temperatures, the challenge on ATRP of 4-VP was overcome by performing the ATRP process at 100 °C. Relatively well-defined poly(γ-benzyl L-glutamate)-*b*-poly(4-vinyl pyridine) diblock copolymers were successfully synthesized and characterized. Upon solvent vapor annealing, thin films of the diblock copolymers showed micro-phase separation behavior.

Keywords: *polyglutamates, poly(4-vinyl pyridine), block copolymer.*

Data Availability: Research data is available upon request from the corresponding author.

How to cite: Truong, T. T., Nguyen, L. T., Doan, T. C. D., Nguyen, L. T. T., & Nguyen, H. T. (2025). Synthesis of well-defined polypeptide-based diblock copolymers. *Polímeros: Ciência e Tecnologia*, *35*(3), e20250031. https://doi.org/10.1590/0104-1428.20240104

1. Introduction

Among vast synthetic polymeric systems, synthetic polypeptides composed of amino acid units have drawn great interests owing to their biocompatibility and biodegradability[1,2]. A wide diversity of synthetic polypeptide structures can be synthesized and modified with various functional groups to interact with biological targets[3]. Their ordered secondary structures (α-helix or β-sheet) as well as ability of organize supramolecularly via abundant electrostatic and hydrogen bond interactions have been utilized to construct macro- and micro-structural architectures[4,5]. Main approaches for synthesizing polypeptides of various α-amino acid monomer units include solution phase coupling, solid phase peptide synthesis and ring opening polymerization (ROP) of α-amino acid N-carboxyanhydrides (NCAs)[6]. The ROP of NCA monomers has been the mostly well-known method to produce high molecular weight polypeptides, in which the reaction initiated via the amine mechanism using a primary amine initiator has been recognized to result in "living" amine chain end[7-9].

Polypeptide-based block copolymers with interesting combined features of biomaterials and self-assembly behavior of polypeptide sequences have been explored for various applications, such as tissue engineering scaffolds[10], drug delivery[11], self-healing[12,13] and antimicrobial applications[14]. To fabricate polypeptide-based block copolymer structures, either different kinds of polypeptides can be incorporated or a polypeptide and a biocompatible synthetic polymer can be combined to meet the requirements for specific applications. Within the wide range of poly(α-amino acid), poly(γ-benzyl-L-glutamate) (PBG), with good biocompatibility and high propensity to adopt the α-helix conformation, has been integrated as an α-helical rod block into different block copolymer designs to form self-assemblies[15]. Bonduelle and coworkers have prepared block copolymers of PBG and poly(γ-propagyl-L-glutamate) followed by functionalization of nucleobases via the copper catalyzed-azide-alkyne cycloaddition (CuAAC) reaction[16]. Other examples of polymers that have been combined with PBG include polysarcosine[17], polyethylene[18], poly(ethylene oxide)[19-22], poly(N-isopropylacryamide)[23], poly(isobutylene)[24], poly(3,4-dihydroxy-L-phenylalanine)[25], poly(L-glutamic acid)[26], poly(2-methacryloyloxyethyl phosphorylcholine)[27], poly(ω-pentadecalactone)[28],

poly(L-phenyl alanine)[29], poly(lysine)[30], polystyrene[31] and elastin-like polypeptide[32].

In this work, we report a straightforward approach to synthesize well-defined diblock copolymers of PBG with poly(4-vinyl pyridine) (Scheme 1). PBG was first obtained via the ROP of the benzyl glutamate NCA monomer under reduced temperature condition to achieve a high content of "amine living chains". PBG with amine end group was modified into an atom transfer radical polymerization (ATRP) macroinitiator to initiate the ATRP polymerization of 4-vinyl pyridine at an enhanced temperature. The performance of the ATRP reaction at a relatively high temperature was found to overcome the problem of low efficacy of the rod polypeptide macroinitiator.

2. Materials and Methods

2.1 Materials

L-glutamic acid (Aldrich, 99%), sulfuric acid (Merck, 96%), trifluoroacetic acid (TFA, Merck, 99%), benzyl alcohol (Acros, 99%), triethylamine (Merck, 99%), triphosgene (Acros, 99%), n-hexylamine (Merck, 99%), α-pinene (Sigma-Aldrich 98%), 4-(chloromethyl)benzoyl chloride (Sigma-Aldrich, 97%), tris(2-aminoethyl)-amine (Acros, 96%), benzyl chloride (Merck, 99%), formaldehyde (Merck, 35%), formic acid (Merck, 37%), NaOH (Merck, 99%), aluminum oxide (Merck, basic), CuCl (Acros, anhydrous, 99%), N,N-dimethylformamide (Acros, extra dry) and Dowex Marathon MSC (Sigma-Aldrich, hydrogen form) were used as received. 4-Vinylpyridine (Aldrich, 95%) was purified with basic Al_2O_3 column prior use. All the solvents (HPLC grade, Fisher Chemicals) were were dried with molecular sieves according to standard procedures.

2.2 Characterizations

^{1}H NMR spectra were recorded in deuterated chloroform ($CDCl_3$) with TMS as an internal reference, on a Bruker Avance 300 at 300 MHz. Attenuated total reflectance (ATR) FT-IR spectra were collected as the average of 128 scans with a resolution of 4 cm^{-1} on a FT-IR Tensor 27 spectrometer equipped with a Pike MIRacle ATR accessory with a diamond/ZnSe element. Gel Permeation Chromatography (GPC) measurements were performed in dimethylformamide with 0.01 mol/L LiBr on a Polymer PL-GPC 50 gel permeation chromatograph system equipped with an RI detector. The data analysis was performed with reference to polystyrene standards. Thermogravimetric analysis (TGA) measurements were performed on a NETZSCH STA 409 PC Instruments with a heating rate of 10 °C/min under N_2 atmosphere. Differential scanning calorimetry (DSC) measurements were performed using a DSC Q20 V24.4 Build 116 calorimeter with the heating and cooling rate of 10.00 °C/min. Atomic force microscopy (AFM) images were obtained using a Bruker Dimension 3100 atomic force microscope.

2.3 Synthesis of γ-benzyl-L-glutamate (BG)

γ-Benzyl-L-glutamate was prepared via Fischer esterification of L-glutamic acid and benzyl alcohol. To a flask containing 30 mL of diethyl ether 6 mL of concentrate sulfuric acid as added dropwise, followed by the addition of 60 mL of benzyl alcohol. Diethyl ether was then removed by rotary evaporation. 8.5 g of L-glutamic acid was added and the mixture was stirred for 24 h at room temperature. 120 mL of ethanol and 50 mL of triethylamine were added slowly to form a white suspension, which was further kept at 5 °C for 24 h. The raw product was collected by filtration and washed with ethanol. After recrystallization from 400 mL of water at 80 °C, the white product was dried under vacuum at 50 °C overnight and was stored at -18 °C. Yield: 65%. ^{1}H-NMR ($CDCl_3$/TFA (10/1, v/v), 300 MHz): δ = 2.106−2.385 (2H, m, CH_2), 2.711 (2H, t, CH_2), 4.169 (1H, s, CH), 5.108 (2H, d, CH_2), 7.216−7.452 (5H, m, phenyl), 7.896 (2H, s, NH_2), 12.4 (TFA).

2.4 Synthesis of γ-benzyl-L-glutamate N-carboxyanhydride (BG-NCA)

2.37 g (0.01 mol) of BG was dissolved in 20 mL of dry tetrahydrofuran, followed by addition of 3.8 mL of α-pinene (0.024 mol, 1.2 eq.) and 1.188 g of triphosgene

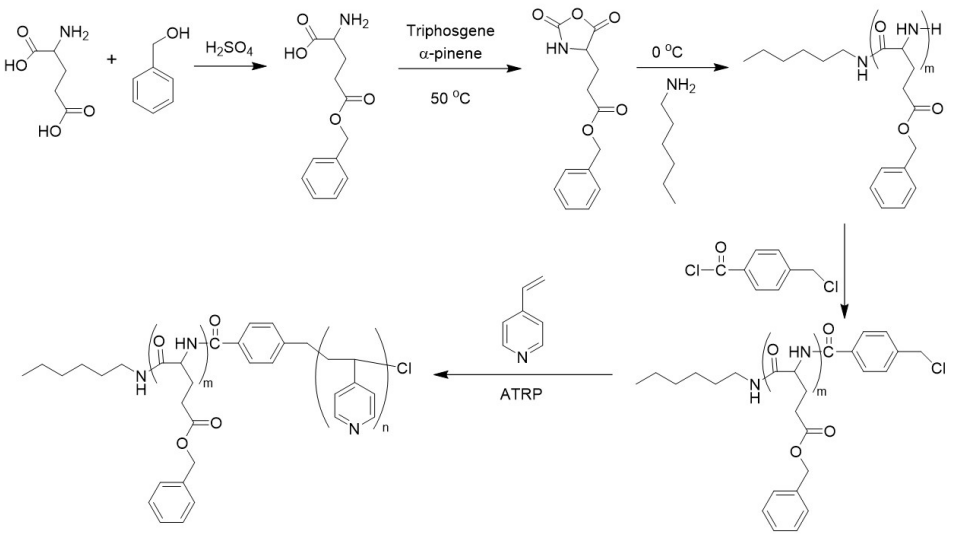

Scheme 1. Controlled synthesis of diblock copolymer PBG-*b*-P4VP.

(0.004 mol, 0.4 eq.). The reaction was performed at 50 °C for 2 h until a clear solution was formed. After that, the raw BG-NCA was filtered and precipitated in 300 mL n-hexane, collected by filtration and dried under vacuum. The raw product was dissolved in tetrahydrofuran and precipitated in n-hexane twice to give a white powder, which was stored under nitrogen atmosphere at -18 °C. ^{1}H-NMR ($CDCl_3$, 300 MHz): δ = 2.010−2.353 (1H, m, CH_2), 2.589 (2H, t, CH_2), 4.377 (1H, t, CH), 5.134 (2H, s, CH_2), 6.675 (1H, s, HN), 7.294─7.452 (5H, m, phenyl).

2.5 Synthesis of poly(γ-benzyl-L-glutamate) (PBG)

PBG was synthesized via ring-opening polymerization of BG-NCA according to the previously reported procedure.[9] Under nitrogen atmosphere, to a solution of BG-NCA in chloroform (5% w/v), at 0 °C, n-hexylamine as initiator was injected and the reaction mixture was stirred for 7 days. 2.367 g of BG-NCA and 47.5 µL of n-hexylamine were used to synthesize PBG1, while 2.367 g of BG-NCA and 23.8 µL of n-hexylamine were used to synthesize PBG2. The product was precipitated into methanol, filtered and dried under vacuum at 50 °C, yielding a white product. Yield: 94−95%. ^{1}H-NMR ($CDCl_3$/TFA (10/1, v/v), 300 MHz): δ = 0.859 (3H, s, CH_3 of initiator), 1.267 (8H, s, CH_2 of initiator), 1.557 (2H, s, CH_2 of initiator), 1.800−2.685 (4H, t, CH_2), 3.945 (1H, s, CH), 5.030 (2H, s, CH_2), 7.118−7.400 (5H, m, phenyl), 8.050−8.490 (1H, s, NH), (TFA).

2.6 End group modification of PBG

To a solution of PBG in dichloromethane (2%, w/v), α-pinene (10 eq. with respect to PBLG) was added. Then, a solution of 4-(chloromethyl)benzoyl in dichloromethane (2%, w/v) was added dropwise. The reaction mixture was stirred at room temperature for 10 h. After the reaction, the product (PBG-Cl) was precipitated in diethyl ether and dried under vacuum at 50 °C overnight, and was stored in dark at -18 °C.

2.7 Synthesis of Me_6TREN

Me_6TREN was synthesized according to the procedure previously reported[33]. To a mixture of 36 mL of formaldehyde (37%) and 45 mL of formic acid in 16 mL of distilled water, 10 mL of tris(2-aminoethyl)-amine was added dropwise. The mixture was stirred for 30 min at room temperature. The reaction was carried out at 120 °C for 6 h. The orange product was distilled by rotary evaporation to remove water and unreacted reactants. 150 mL of NaOH solution (20% w/v) was added until pH = 10. The oily layer at the bottom was extracted by dichloromethane. After the solvent and other low boiling temperature contaminants were removed by rotary evaporation, the final product was obtained by Kugelrohr distillation (130 °C, 0.2 mbar) as a clear, colorless and oil-like liquid. Me_6TREN was stored at 4 °C under nitrogen atmosphere. ^{1}H-NMR (ppm): δ = 2.213 (18H, s, CH_3), 2.323−2.400 (6H, m, CH_2), 2.553−2.636 (6H, m, CH_2).

2.8 Synthesis of homopolymer poly(4-vinyl pyridine) (P4VP)

P4VP was synthesized via the ATRP of 4-vinylpyridine (4-VP) from the initiator. 0.0198 g (0.2 mmol) of CuCl was dissolved in 1.1 mL of anhydrous dimethylformamide (DMF) under nitrogen atmosphere, followed by the addition of 2.2 mL (20.6 mmol) of 4-VP and 52.6 µL (0.2 mmol) of Me_6TREN. The temperature was increased to 50 °C and 6 µL (0.052 mmol) of benzyl chloride was injected. The reaction was carried out at 50 °C overnight. After the reaction, the reaction mixture was diluted with 30 mL of DMF. The product was precipitated into diethyl ether, filtered and dried under vacuum a 50 °C. Yield: 87.4%. For removal of CuCl, a solution of the product in chloroform (2%, w/v) was mixed with Dowex Marathon MSC hydrogen form ion exchange resin at room temperature for 20 h. Copper elemental analysis: < 3.0 ppm. ^{1}H-NMR ($CDCl_3$, 300 MHz): δ = 0.970−2.226 (3H, m, CH_2CH), 5.932−6.647 (2H, d, pyridine), 8.318 (2H, s, pyridine). M_n (GPC) = 61000, Đ (GPC) = 1.2.

2.9 Synthesis of diblock copolymer poly(γ-benzyl-L-glutamate)-b-poly(4-vinyl pyridine) (PBG-b-P4VP)

For *PBG1-b-P4VP*, 0.243 g (0.05 mmol) of PBGl_Cl, 9.9 mg (0.1 mmol) of CuCl, 26.3 µL (0.1 mmol) of Me6TREN dissolved in 2.16 mL of dry DMF were used. For *PBG2-b-P4VP,* 1.21 g (0.1 mmol) of PBGl_Cl, 19.8 mg (0.2 mmol) of CuCl, 52.6 µL (0.2 mmol) of Me6TREN dissolved in 4.3 mL of dry DMF were used. *Procedure*: In a dry flask under nitrogen atmosphere, PBGl_Cl and CuCl were added. Then, a solution of Me_6TREN in dry DMF was injected to the flask, followed by the injection of 2.16 mL (0.02 mol) of 4-vinylpyridine. The flask was stirred at 100 °C for 12 h. After the reaction mixture was cooled down, the reaction mixture was diluted by adding 25 mL of DMF and precipitated in 500 mL of diethyl ether. A solution of the raw product in chloroform (2%, w/v) was mixed with Dowex Marathon MSC hydrogen form ion exchange resin at room temperature for 20 h to remove CuCl. Then, the copolymer product was precipitated in toluene twice. The received product was dried under vacuum overnight. Yield: 65−70%.

3. Results and Discussion

The BG and BG-NCA monomers were synthesized according to previous procedures[34]. PBG was synthesized via ring-opening polymerization of BG-NCA using the "living" process reported by Schué and coworkers[9]. Conducting the polymerization at 0 °C has been addressed to suppress significant side reactions, resulting in "living" amine chain ends[35]. Two polymers with designed degrees of polymerization (DPs) of 25 and 50 were prepared and named as PBG1 and PBG2, respectively. Figure 1 presents the ^{1}H NMR spectra of BG, BG-NCA, PBG1 and PBG 2, with all the peaks characteristic of their structures. The formation of the NCA ring structure is confirmed by the peak at 6.7 ppm attributed to the amide NH proton and the peak at 4.4 ppm ascribed to the ring methine (CH) proton. The structure of BG and BG-NCA was further confirmed by FT-IR analysis (Figure 2). The FT-IR spectrum of BG showed a very broad vibrational absorption region of overlapping bands in the range of 3033-2600 cm^{-1} attributed to acid O-H and NH_2 stretches, an acid C=O stretching band at 1577 cm^{-1}, a benzyl ester C=O stretching band at 1722 cm^{-1} and a band at 730 cm^{-1} ascribed to the aromatic C-H out-of-plane bending vibration.

The formation of BG-NCA structure was supported by the disappearance of the broad band regions corresponding to (CO)O-H and NH2 vibrations, and the appearance of characteristic absorption bands at ~3250 cm^{-1} (amide N-H stretch), 1771 cm^{-1} (anhydride carbonyl symmetric stretch), 1726 cm^{-1} (benzyl ester C=O stretch), 1701 cm^{-1} (amide I).

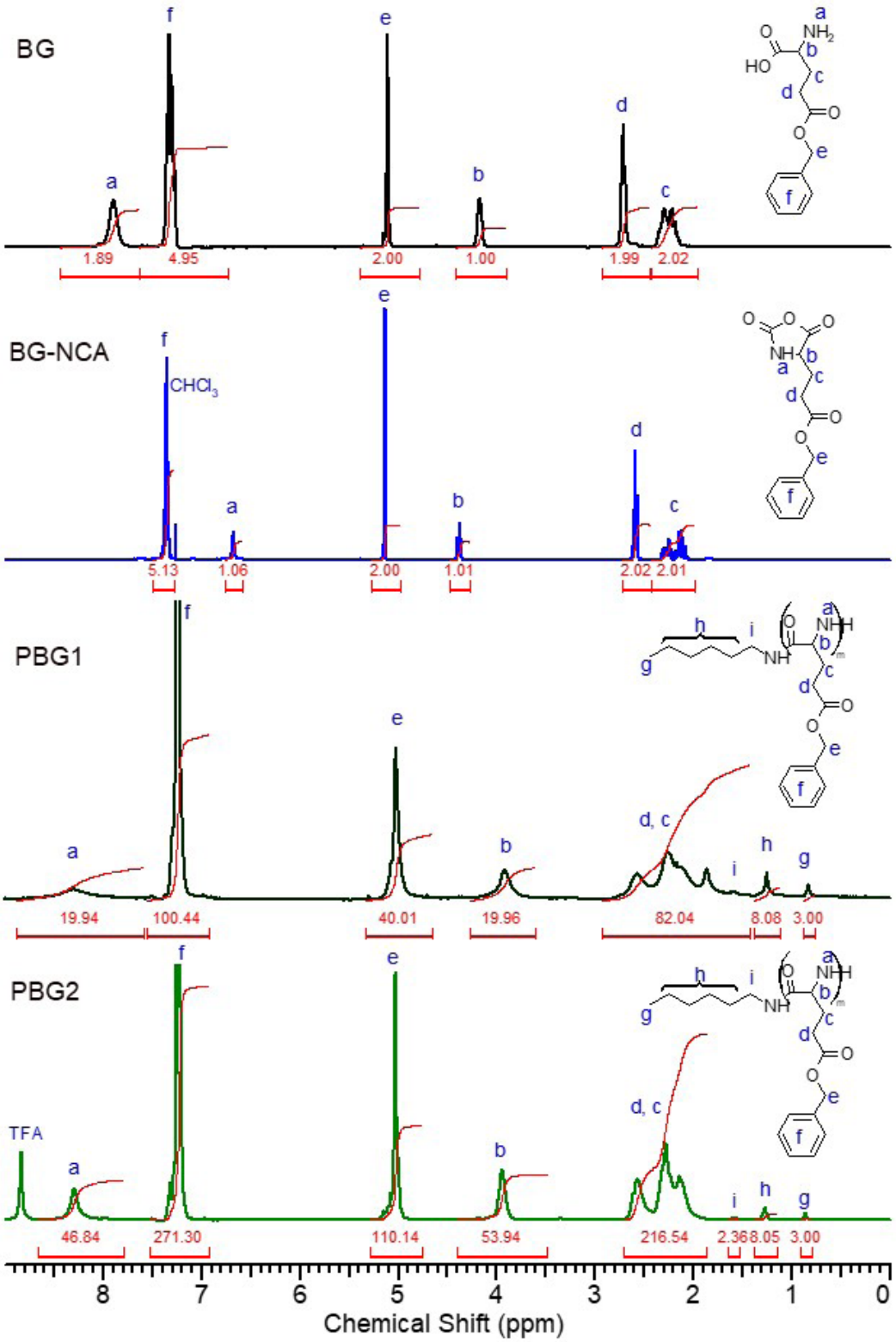

Figure 1. ^{1}H NMR spectra of BG, BG-NCA, PBG1 and PBG2.

The ^{1}H NMR spectra of the resulting polymers PBG1 and PBG2 also revealed peaks typical of the polymer structure, with shift of the amide NH peak to 8.3 (Figure 1, PBG1). In the presence of a few drops of TFA to eliminate aggregation of polymer chains, the amide NH signal at 8.3 ppm became sharper (Figure 1, PBG2). By comparing the integral ratio between peak b at 4.4 ppm (ring methine) and g at 0.86 ppm (CH_3 of the n-hexyl end group), DPs values of 21 (M_n = 4601) and 54 (M_n = 11840) were determined for PBG1 and PBG2, respectively. The GPC results gave just slightly higher values of M_n of 6600 and 13200 g mol^{-1} and Đ values of 1.23 and 1.26 for PBG1 and PBG2, respectively (Table 1). The good agreement between the resulting and designed molecular weights suggested a relatively controlled NCA-ring opening polymerization process was obtained. PBGs were further coupled with 4-(chloromethyl)benzoyl chloride to give polymers (named as PBG1_Cl and PBG2_Cl) end-capped with (chloromethyl)benzoyl group that can be used as an initiating group for the ATRP process. According the chloride analysis results of PBG_Cl polymers, capping efficiencies of 76.9 and 82.1% for PBG1_Cl and PBG2_Cl, respectively.

PBG-*b*-P4VP was then synthesized via the ATRP of 4-vinyl pyridine (4-VP) from the macroinitiator PBG-Cl. PBG-Cl and CuCl were dissolved in anhydrous dimethylformamide (DMF), followed by the addition of 4-VP and Me_6TREN. The temperature was increased to 100 °C and the reaction was left overnight. It should be noted that the ATRP of 4VP using PBG_Cl as macroinitiator at room temperature and at 50 °C did not result any trace of P4VP block. After the reaction, the diblock copolymer product was recovered by precipitation into diethyl ether to eliminate the unreacted 4VP monomers. The copolymer was further purified by double precipitation in toluene, which is a good solvent for PBG but a poor solvent for P4VP and its copolymers. Therefore, the unreacted PBG polymer could be removed. In a comparison of the ^{1}H NMR spectra of the diblock copolymers with that of PBG1_Cl, new peaks attributed to the pyridine ring protons at ~8.3 and 6.4 ppm and to the backbone methylene and methine protons at around 2.8−0.8 ppm of P4VP block were observed (Figure 3). By comparing the integral ratio between the peak corresponding to the pyridine ring (peak x or y, Figure 3) and the peak arising from the methine proton of the PBG block (peak b, Figure 3), the ratio between the DPs of two blocks were estimated. Taking into consideration of the DPs of PBG1 and PBG2 (determined by ^{1}H NMR), DPs values of the P4VP block were determined to be 399 and 168 for PBG1-*b*-P4VP and PBG2-*b*-P4VP, respectively.

Figure 4 compares the GPC curves of the diblock copolymers with those of corresponding macroinitiators. The GPC curves of the copolymers clearly shifted to the higher molecular weight values, indicating the successful formation of the diblock copolymer structure. The GPC results also showed acceptable molecular weight distribution (Đ) values of 1.46 and 1.66 for PBG1-*b*-P4VP and PBG2-*b*-P4VP, respectively (Table 1).

Figure 5 compares the FT-IR spectra of the homopolymers PBG and P4VP with those of diblock copolymers PBG1-*b*-P4VP and PBG2-*b*-P4VP. The structure of the polypeptide

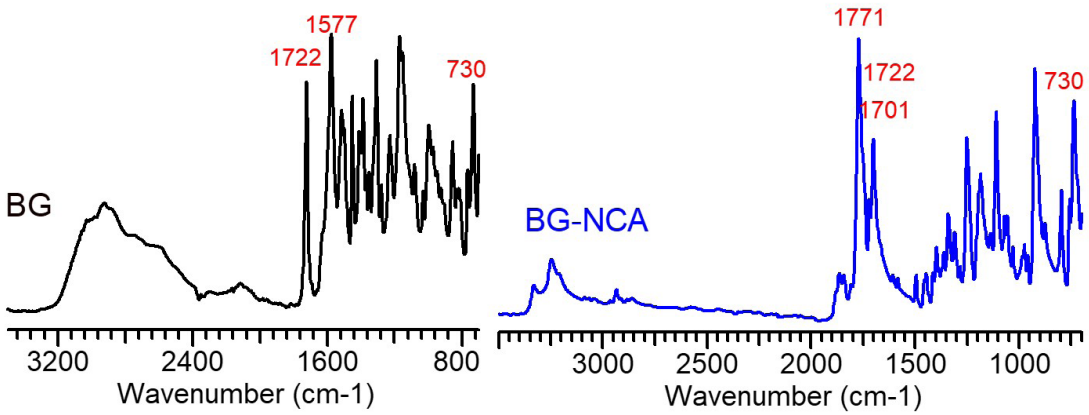

Figure 2. FT-IR spectra of BG and BG-NCA.

Table 1. Molecular weight characteristics of PBGs and PBG-*b*-P4VPs.

Polymers	DP of PBG (designed)[a]	DP of P4VP (designed)[a]	Efficacy of macroinitiator[b]	Yield	DP of P4VP (theoretical)[c]	DP of PBG (NMR)	DP of P4VP (NMR)	M_n of polymer/ copolymer (NMR)	M_n (GPC)	Đ (GPC)
PBG1	25		76.9%	94%		21		4604	6600	1.23
PBG1-*b*-P4VP		400		70%	364		399	46,669	60,800	1.46
PBG2	50		82.1%	95%		54		11840	13200	1.26
PBG2-*b*-P4VP		200		65%	158		168	29,506	32000	1.66

[a]calculated from monomer and initiator/macroinitiator feed ratio; [b]from chloride elemental analysis of PBG_Cl; [c]calculated taking into account the efficacy of macroinitiator and yield of polymerization of 4VP.

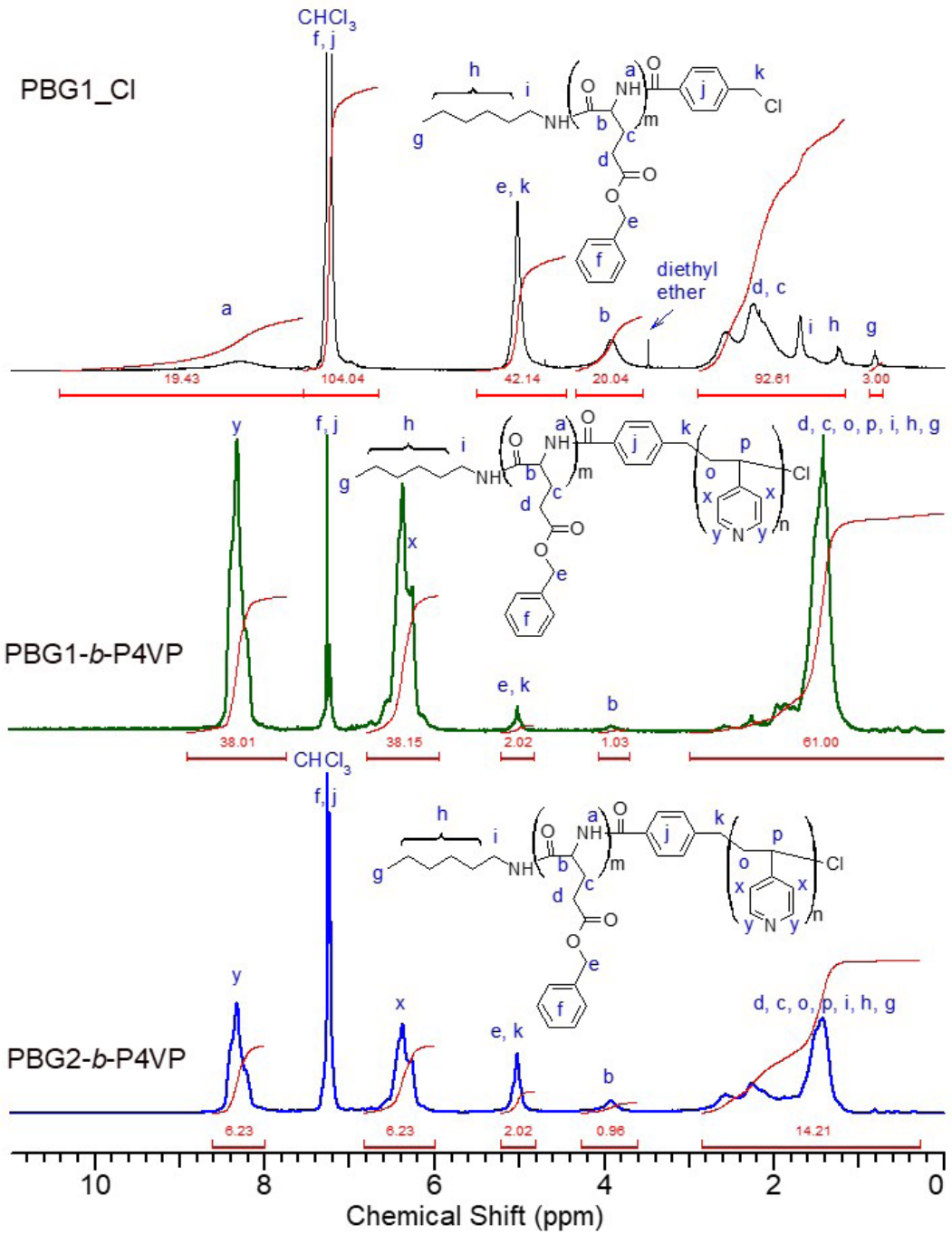

Figure 3. ^{1}H NMR spectra of PBG1_Cl, PBG1-*b*-P4VP and PBG2-*b*-P4VP.

PBG was again confirmed by FT-IR analysis, as indicated by characteristic vibrational absorption bands of amide and ester groups at 3293 cm-1 (amide A), 1728 (ester C=O stretch), 1650 cm-1 (a5mide I) and 1543 (amide II). The FT-IR spectrum of P4VP revealed vibrational absorption bands typical of the pyridine ring, including bands at 1596-1556 cm^{-1} (doublet, pyridine ring stretches), 993 cm^{-1} (pyridine ring breathing mode) and 818 cm^{-1} (pyridine C-H out-of-plane deformation).

The differential scanning calorimetry (DSC) heating and cooling scans of the PBG and P4VP homopolymers showed glass transitions at 15.3 and 154.3 °C, respectively (Figure 6). For PBG1-*b*-P4VP, due to the large length of the P4VP block (DP of P4VP = 399) relative to the PBG block (DP of PBG = 21), only a glass transition attributed to the P4VP block was detectable at a somewhat lower temperature of 149.6 °C. On the other hand, the DSC result of PBG2-*b*-P4VP revealed both glass transitions related to both PBG and

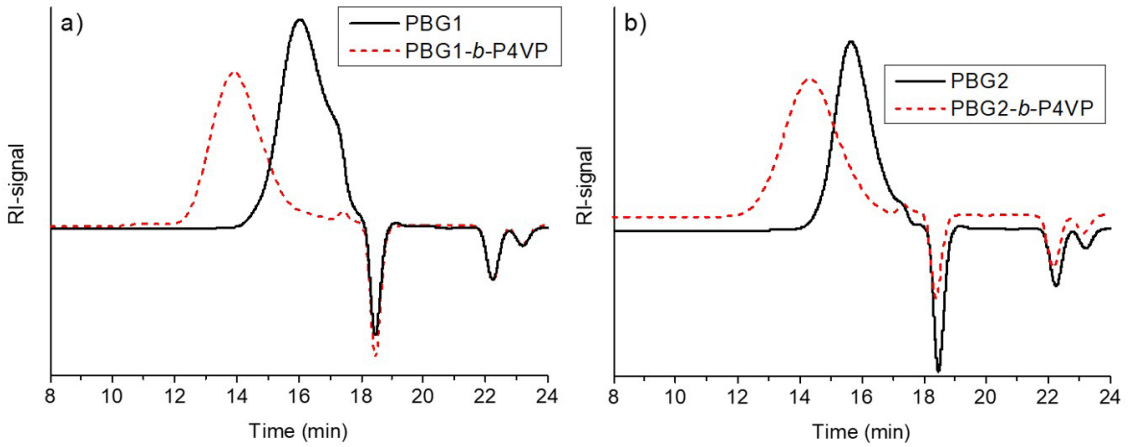

Figure 4. GPC curves of PBG1 and PBG1-*b*-P4VP (a), and of PBG2 and PBG2-*b*-P4VP (b).

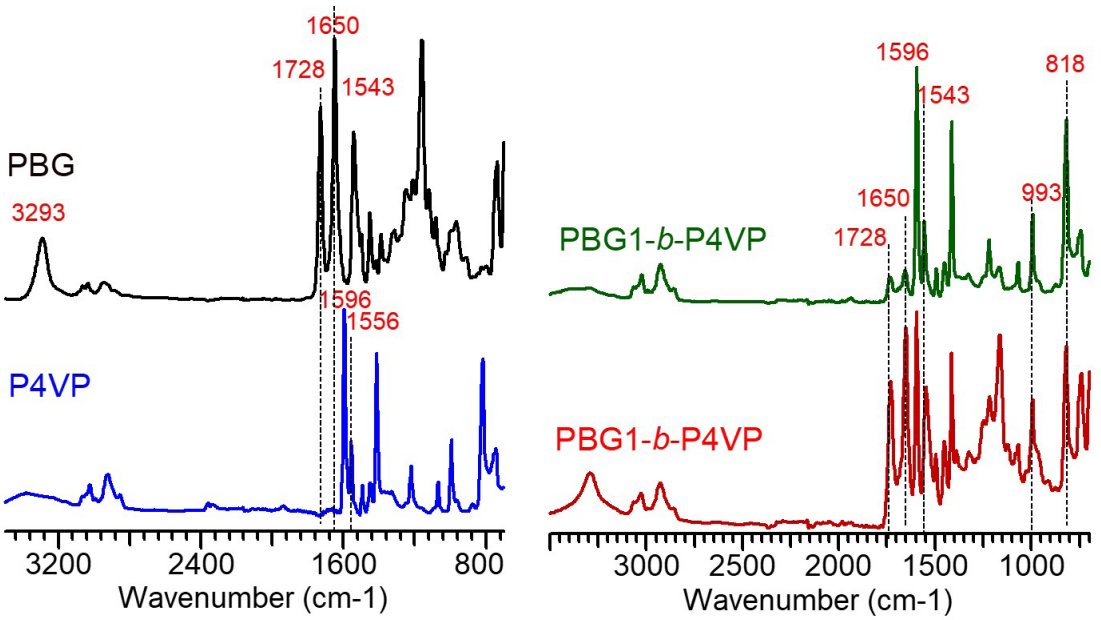

Figure 5. FT-IR spectra of PBG, P4VP, PBG1-*b*-P4VP and PBG2-*b*-P4VP.

P4VP blocks at 15.5 and 136.5 °C, respectively, indicating the diblock copolymer structure. The clearly lower glass transition temperature of P4VP block in PBG2-*b*-P4VP compared with that of the P4VP homopolymer could arise from hydrogen bonding interactions between the two blocks.

The thermogravimetric analysis (TGA) results showed that while P4VP was thermally stable up to 325 °C, PBG started to degrade at 265 °C (Figure 7). However, PBG had a relatively high char yield of 14.2% where as P4VP decomposed completely. The TGA curves of the diblock copolymers revealed a two-step degradation process corresponding to consecutive decompositions of the PBG block and P4VP block. The weight loss of the first degradation step and the char yield was well relevant to the weight fraction of the PBG block in the diblock copolymers (Table 2).

Thin films of the diblock copolymers were prepared on silicon wafers via spin-coating and their morphologies were investigated by atomic force microscopy (AFM). As shown in Figure 8a, the film matrix of the film matrix PBG1-*b*-P4VP before annealing was quite flat and homogeneous. Some round holes with different diameters were distributed randomly. The reason of forming these holes is still not clear. The ring-in-ring structure in the right and left corners might be due to fast, inhomogeneous evaporation of the solvent, as the domains inside and outside the rings had the same height and composition. Interestingly, after annealing with the vapor of chloroform as a good solvent, the hole structure disappeared, and there appeared some white, drop-like domains embedded in the matrix. The edges of the drop-like domains were rather sharp. Taking the phase image into account (Figure 8a-D),

Table 2. Weight loss and char yield values obtained from the TGA results.

	Weigh fraction of PBG block[a]	Weight loss at 340 °C	Char yield_theoretical[b]	Char yield_TGA
PBG1-*b*-P4VP	10%	12%	1.4%	2.1%
PBG2-*b*-P4VP	40%	41%	5.7%	7.3%

[a]calculated from the Mn values determined by ^{1}H NMR method (Table 1); [b]calculated from the char yield of the PBG homopolymer and the weight fraction of the PBG block in the diblock copolymers.

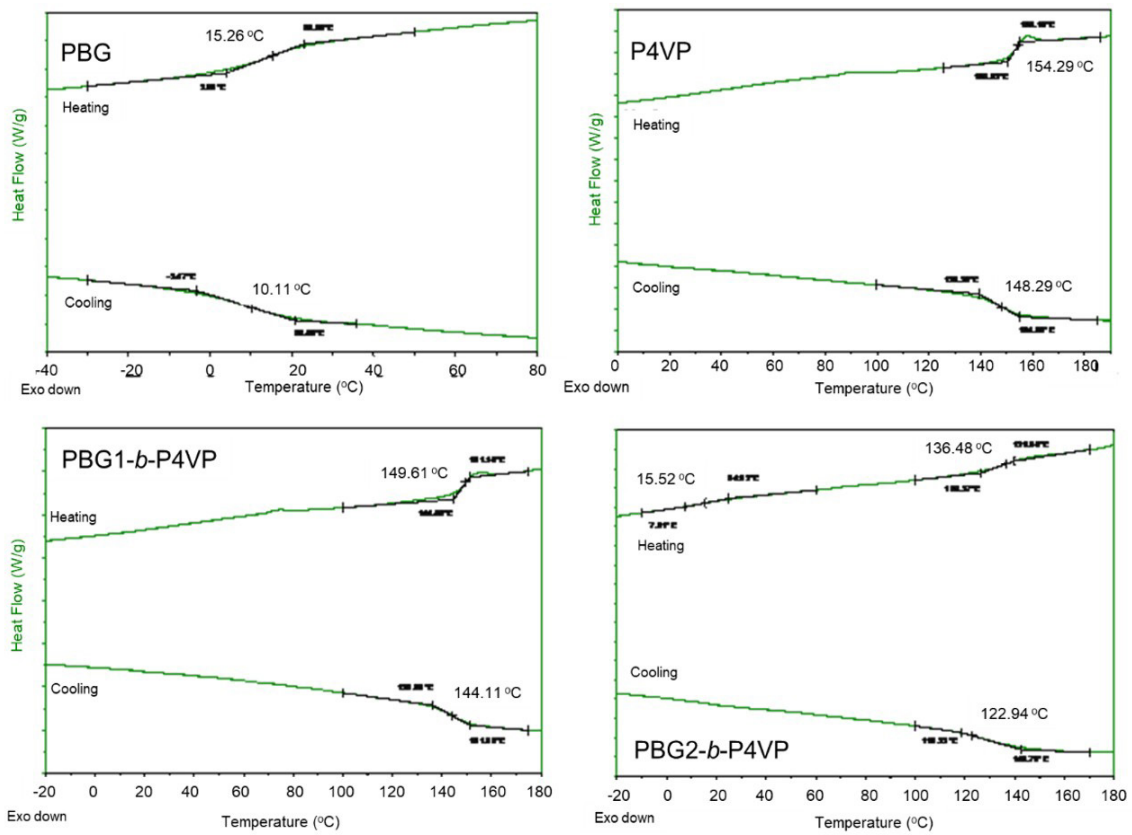

Figure 6. DSC thermograms of PBG, P4VP, PBG1-*b*-P4VP and PBG2-*b*-P4VP.

it is very clear that the drop-like domain belonged to the PBG block and the matrix was formed of the P4VP block. The explanation for this could be that the PBG helices were much more rigid than P4VP coil chains and during the solvent annealing process, the helices remained intact while P4VP coils were swollen.

The AFM images of PBG2-*b*-P4VP are shown in Figure 8b. Before annealing (Figure 8b-A and B), the film surface had an island-like structure. These "islands" had a higher boundary but lower inside domain, and their sizes were not uniform. This was probably due to relatively broader polydispersity (Đ = 1.66) of PBG2-*b*-P4VP. After chloroform vapor annealing, phase separation became more obvious. From the topographic image (Figure 8b-C), it was clear that instead of the island-like structure, an inhomogeneous network was formed. For both copolymers, drop-like and round-like domains after long-time annealing process converted to partly orientated "worm-like" domains of rod-like PBG block situated in the matrix of coil-like

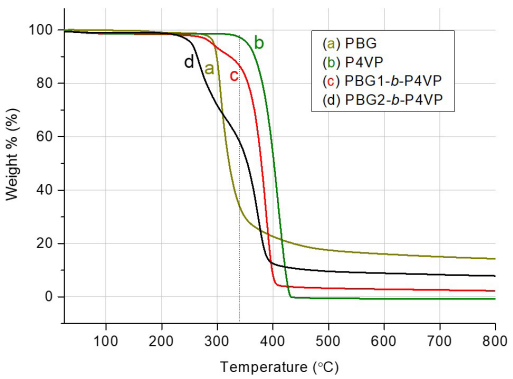

Figure 7. TGA curves of PBG, P4VP, PBG1-*b*-P4VP and PBG2-*b*-P4VP.

P4VP block. It indicates that during the annealing process, phase rearrangement occurred.

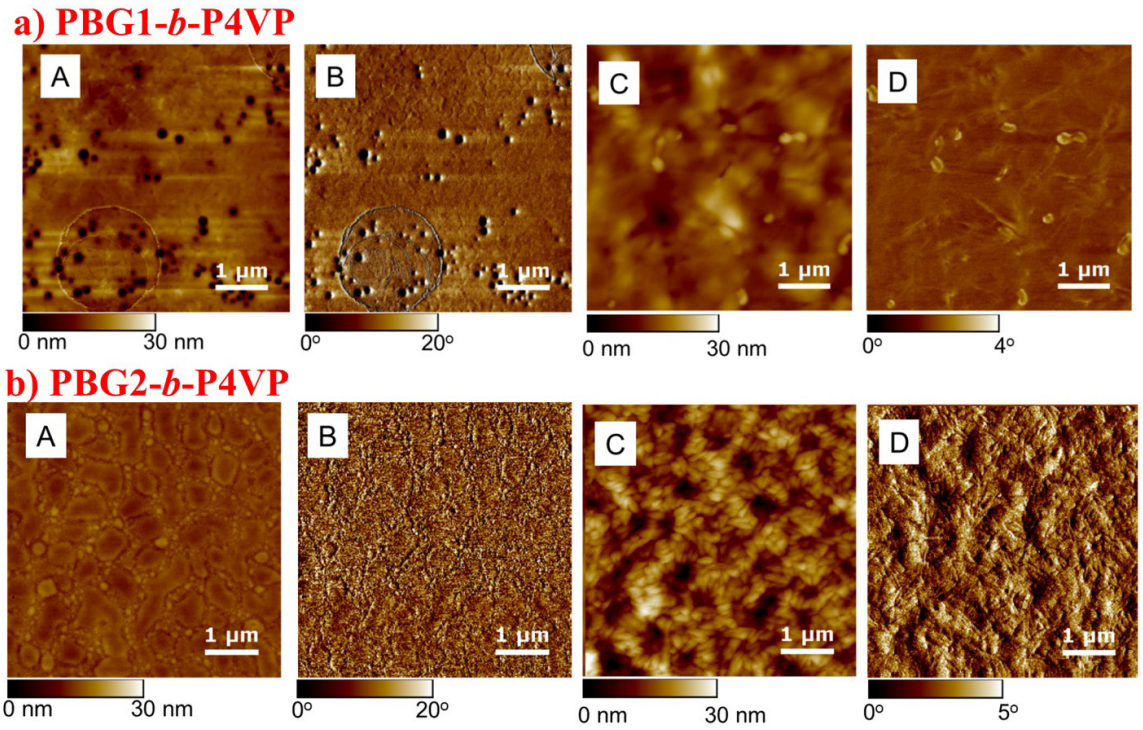

Figure 8. AFM images (5 µm × 5 µm) of PBG1-*b*-P4VP (a) and PBG2-*b*-P4VP (b) before annealing (A: topographic image, B: phase image) and after 3-day-chloroform vapor annealing (C: topographic image, D: phase image).

4. Conclusion

Two PBG-*b*-P4VP diblock copolymers with different block length ratios were successfully synthesized through "living" NCA ring-opening polymerization at 0 °C in combination with ATRP in DMF at 100 °C. Their chemical structures were confirmed by ^{1}H-NMR, and ATR-FTIR. Their molecular weights and thermal properties were characterized by GPC, TGA and DSC. In addition, the AFM results of thin films of the diblock copolymers proved that solvent annealing rearranged phase domains prompting micro-phase separation.

5. Author's Contribution

- **Conceptualization –** Le-Thu Thi Nguyen.
- **Data curation –** NA.
- **Formal analysis –** NA.
- **Funding acquisition –** Thuy Thu Truong.
- **Investigation –** Thuy Thu Truong.
- **Methodology –** Luan Thanh Nguyen; Tin Chanh Duc Doan; Ha Tran Nguyen.
- **Project administration –** Ha Tran Nguyen; Thuy Thu Truong.
- **Resources –** Ha Tran Nguyen.
- **Software –** NA.
- **Supervision –** Ha Tran Nguyen.
- **Validation –** Luan Thanh Nguyen; Tin Chanh Duc Doan; Ha Tran Nguyen.
- **Visualization –** NA.
- **Writing – original draft –** Thuy Thu Truong; Luan Thanh Nguyen.
- **Writing – review & editing –** Luan Thanh Nguyen; Tin Chanh Duc Doan; Le-Thu Thi Nguyen; Ha Tran Nguyen.

6. Acknowledgements

This research is funded by Vietnam National University Hochiminh City (VNU-HCM) under grant number: TX2025-20a-01.

7. References

1. Wang, T.-T., Xia, Y.-Y., Gao, J.-Q., Xu, D.-H., & Han, M. (2021). Recent progress in the design and medical application of in situ self-assembled polypeptide materials. *Pharmaceutics*, *13*(5), 753. http://doi.org/10.3390/pharmaceutics13050753. PMid:34069645.
2. Zhang, P., Li, M., Xiao, C., & Chen, X. (2021). Stimuli-responsive polypeptides for controlled drug delivery. *Chemical Communications (Cambridge)*, *57*(75), 9489-9503. http://doi.org/10.1039/D1CC04053G. PMid:34546261.
3. Lin, M., & Sun, J. (2022). Antimicrobial peptide-inspired antibacterial polymeric materials for biosafety. *Biosafety and Health*, *4*(4), 269-279. http://doi.org/10.1016/j.bsheal.2022.03.009.
4. Liu, Y., Tang, H., Zhu, M., Zhu, H., & Hao, J. (2022). Controlling self-assembly of co-polypeptide by block ratio and block sequence. *Polymer*, *254*, 125093. http://doi.org/10.1016/j.polymer.2022.125093.
5. Abdelghani, M., Shao, J., Le, D. H. T., Wu, H., & van Hest, J. C. M. (2021). Self-assembly or coassembly of multiresponsive

histidine-containing elastin-like polypeptide block copolymers. *Macromolecular Bioscience*, *21*(6), e2100081. http://doi.org/10.1002/mabi.202100081. PMid:33942499.

6. Liu, Y., Li, D., Ding, J., & Chen, X. (2020). Controlled synthesis of polypeptides. *Chinese Chemical Letters*, *31*(12), 3001-3014. http://doi.org/10.1016/j.cclet.2020.04.029.
7. Badreldin, M., Salas-Ambrosio, P., Ayala, M., Harrisson, S., & Bonduelle, C. (2024). Synthesis of Polypeptides by ring-opening polymerization: a concise review. *Current Organic Chemistry*, *28*(15), 1154-1163. http://doi.org/10.2174/0113852728274519240228105518.
8. Rasines Mazo, A., Allison-Logan, S., Karimi, F., Chan, N. J.-A., Qiu, W., Duan, W., O'Brien-Simpson, N. M., & Qiao, G. G. (2020). Ring opening polymerization of α-amino acids: advances in synthesis, architecture and applications of polypeptides and their hybrids. *Chemical Society Reviews*, *49*(14), 4737-4834. http://doi.org/10.1039/C9CS00738E. PMid:32573586.
9. Vayaboury, W., Giani, O., Cottet, H., Deratani, A., & Schué, F. (2004). Living Polymerization of α-Amino Acid N-Carboxyanhydrides (NCA) upon Decreasing the Reaction Temperature. *Macromolecular Rapid Communications*, *25*(13), 1221-1224. http://doi.org/10.1002/marc.200400111.
10. Zhao, D., Rong, Y., Li, D., He, C., & Chen, X. (2023). Thermo-induced physically crosslinked polypeptide-based block copolymer hydrogels for biomedical applications. *Regenerative Biomaterials*, *10*, rbad039. http://doi.org/10.1093/rb/rbad039.
11. Wang, X., Song, Z., Wei, S., Ji, G., Zheng, X., Fu, Z., & Cheng, J. (2021). Polypeptide-based drug delivery systems for programmed release. *Biomaterials*, *275*, 120913. http://doi.org/10.1016/j.biomaterials.2021.120913. PMid:34217020.
12. Wang, K.-H., Liu, C.-H., Tan, D.-H., Nieh, M.-P., & Su, W.-F. (2024). Block sequence effects on the self-assembly behaviors of polypeptide-based penta-block copolymer hydrogels. *ACS Applied Materials & Interfaces*, *16*(5), 6674-6686. http://doi.org/10.1021/acsami.3c18954. PMid:38289014.
13. Cai, L., Liu, S., Guo, J., & Jia, Y.-G. (2020). Polypeptide-based self-healing hydrogels: design and biomedical applications. *Acta Biomaterialia*, *113*, 84-100. http://doi.org/10.1016/j.actbio.2020.07.001. PMid:32634482.
14. Maurya, D., Nisal, R., Ghosh, R., Kambale, P., Malhotra, M., & Jayakannan, M. (2023). Fluorophore-tagged poly(ι-Lysine) block copolymer nano-assemblies for real-time visualization and antimicrobial activity. *European Polymer Journal*, *183*, 111754. http://doi.org/10.1016/j.eurpolymj.2022.111754.
15. Ma, T.-L., Yang, S.-C., Cheng, T., Chen, M.-Y., Wu, J.-H., Liao, S.-L., Chen, W.-L., & Su, W.-F. (2022). Exploration of biomimetic poly(γ-benzyl-l-glutamate) fibrous scaffolds for corneal nerve regeneration. *Journal of Materials Chemistry. B, Materials for Biology and Medicine*, *10*(33), 6372-6379. http://doi.org/10.1039/D2TB01250B. PMid:35950376.
16. Nguyen, M., Ferji, K., Lecommandoux, S., & Bonduelle, C. (2020). Amphiphilic nucleobase-containing polypeptide copolymers: synthesis and self-assembly. *Polymers*, *12*(6), 1357. http://doi.org/10.3390/polym12061357. PMid:32560277.
17. Lebleu, C., Plet, L., Moussy, F., Gitton, G., Da Costa Moreira, R., Guduff, L., Burlot, B., Godiveau, R., Merry, A., Lecommandoux, S., Errasti, G., Philippe, C., Delacroix, T., & Chakrabarti, R. (2023). Improving aqueous solubility of paclitaxel with polysarcosine-*b*-poly(γ-benzyl glutamate) nanoparticles. *International Journal of Pharmaceutics*, *631*, 122501. http://doi.org/10.1016/j.ijpharm.2022.122501. PMid:36529355.
18. Lu, Y., Liu, D., Wei, X., Song, J., Xiao, Q., Du, K., Shi, X., & Gao, H. (2023). Synthesis and thermoreversible gelation of coil–rod copolymers with a dendritic polyethylene core and multiple helical poly(γ-benzyl-l-glutamate) arms. *Polymers*, *15*(22), 4351. http://doi.org/10.3390/polym15224351. PMid:38006076.
19. Alsehli, M., & Gauthier, M. (2023). Influence of the core branching density on drug release from arborescent poly(γ-benzyl l-glutamate) end-grafted with poly(ethylene oxide). *International Journal of Translational Medicine*, *3*(4), 496-515. http://doi.org/10.3390/ijtm3040035.
20. Lin, X., He, X., Hu, C., Chen, Y., Mai, Y., & Lin, S. (2016). Disk-like micelles with cylindrical pores from amphiphilic polypeptide block copolymers. *Polymer Chemistry*, *7*(16), 2815-2820. http://doi.org/10.1039/C6PY00152A.
21. Ji, S., Xu, L., Fu, X., Sun, J., & Li, Z. (2019). Light- and metal ion-induced self-assembly and reassembly based on block copolymers containing a photoresponsive polypeptide segment. *Macromolecules*, *52*(12), 4686-4693. http://doi.org/10.1021/acs.macromol.9b00475.
22. El-Mahdy, A. F. M., Yu, T. C., Mohamed, M. G., & Kuo, S.-W. (2021). Secondary structures of polypeptide-based diblock copolymers influence the microphase separation of templates for the fabrication of microporous carbons. *Macromolecules*, *54*(2), 1030-1042. http://doi.org/10.1021/acs.macromol.0c01748.
23. Sang, X., Yang, Q., Wen, Q., Zhang, L., & Ni, C. (2019). Preparation and controlled drug release ability of the poly[N-isopropylacryamide-co-allyl poly(ethylene glycol)]-*b*-poly(γ-benzyl-l-glutamate) polymeric micelles. *Materials Science and Engineering C*, *98*, 910-917. http://doi.org/10.1016/j.msec.2019.01.056. PMid:30813098.
24. Spyridakou, M., Tsimenidis, K., Gkikas, M., Steinhart, M., Graf, R., & Floudas, G. (2022). Effects of nanometer confinement on the self-assembly and dynamics of poly(γ-benzyl-l-glutamate) and its copolymer with poly(isobutylene). *Macromolecules*, *55*(7), 2615-2626. http://doi.org/10.1021/acs.macromol.2c00077.
25. Zhang, Y., Song, W., & Kim, I. (2019). Mussel-Inspired Poly(3,4-dihydroxy-L-phenylalanine)-Block-Poly(γ-benzyl-L-glutamate) bioconjugate-assisted green synthesis of silver nanoparticles. *Journal of Nanoscience and Nanotechnology*, *19*(10), 6559-6564. http://doi.org/10.1166/jnn.2019.17075. PMid:31026993.
26. Lavilla, C., Byrne, M., & Heise, A. (2016). Block-sequence-specific polypeptides from α-Amino Acid N-carboxyanhydrides: synthesis and influence on polypeptide properties. *Macromolecules*, *49*(8), 2942-2947. http://doi.org/10.1021/acs.macromol.6b00498.
27. Liu, G., Zhuang, W., Chen, X., Yin, A., Nie, Y., & Wang, Y. (2016). Drug carrier system self-assembled from biomimetic polyphosphorycholine and biodegradable polypeptide based diblock copolymers. *Polymer*, *100*, 45-55. http://doi.org/10.1016/j.polymer.2016.08.012.
28. Tinajero-Díaz, E., Ilarduya, A. M., & Muñoz-Guerra, S. (2019). Synthesis and properties of diblock copolymers of ω-pentadecalactone and α-amino acids. *European Polymer Journal*, *116*, 169-179. http://doi.org/10.1016/j.eurpolymj.2019.04.009.
29. Jacobs, J., Gathergood, N., Heuts, J. P. A., & Heise, A. (2015). Amphiphilic glycosylated block copolypeptides as macromolecular surfactants in the emulsion polymerization of styrene. *Polymer Chemistry*, *6*(25), 4634-4640. http://doi.org/10.1039/C5PY00548E.
30. Gauche, C., & Lecommandoux, S. (2016). Versatile design of amphiphilic glycopolypeptides nanoparticles for lectin recognition. *Polymer*, *107*, 474-484. http://doi.org/10.1016/j.polymer.2016.08.077.
31. Wang, Y., & Ling, J. (2015). Synthetic protocols toward polypeptide conjugates via chain end functionalization after RAFT polymerization. *RSC Advances*, *5*(24), 18546-18553. http://doi.org/10.1039/C4RA17094F.
32. Le Fer, G., Portes, D., Goudounet, G., Guigner, J.-M., Garanger, E., & Lecommandoux, S. (2017). Design and self-assembly of PBLG-*b*-ELP hybrid diblock copolymers based on synthetic and

elastin-like polypeptides. *Organic & Biomolecular Chemistry*, *15*(47), 10095-10104. http://doi.org/10.1039/C7OB01945A. PMid:29170769.

33. Queffelec, J., Gaynor, S. G., & Matyjaszewski, K. (2000). Optimization of atom transfer radical polymerization using Cu(I)/Tris(2-(dimethylamino)ethyl)amine as a catalyst. *Macromolecules*, *33*(23), 8629-8639. http://doi.org/10.1021/ma000871t.
34. Daly, W. H., & Poché, D. (1988). The preparation of N-carboxyanhydrides of α-amino acids using bis(trichloromethyl) carbonate. *Tetrahedron Letters*, *29*(46), 5859-5862. http://doi.org/10.1016/S0040-4039(00)82209-1.
35. Habraken, G. J. M., Wilsens, K. H. R. M., Koning, C. E., & Heise, A. (2011). Optimization of N-carboxyanhydride (NCA) polymerization by variation of reaction temperature and pressure. *Polymer Chemistry*, *2*(6), 1322-1330. http://doi.org/10.1039/c1py00079a.

Received: Nov. 25, 2024
Revised: Mar. 31, 2025
Accepted: May 06, 2025

Associate Editor: César L. Petzhold